

1 Short title: Reporter system for transcription factor complex DNA interactions

2

3 Author for contact:

4 Ben F. Holt III

5 Scientific Leadership

6 AgBiome

7 Research Triangle, NC 27709

8

DIMR, a Yeast-Based Synthetic Reporter System for Probing Oligomeric Transcription Factor DNA Binding

Zachary A. Myers, Swadhin Swain, Shannan Bialek, Samuel Keltner, and Ben F. Holt III

Department of Microbiology and Plant Biology, University of Oklahoma, Norman, OK, USA

One sentence summary: The DIMR system provides an accessible and easy-to-use platform to elucidate DNA binding and transcriptional regulatory capacity of oligomeric transcription factor complexes

Author contributions: BH and ZM conceived the project. ZM conducted the majority of the data collection, performed all of the data analysis, and wrote the manuscript. SS assisted with protein work, while SB and SK assisted with cloning and some data collection. BH supervised the project and was responsible for funding acquisition and manuscript editing.

Funding information: Funding was provided by an EAGER grant from the National Science Foundation (MCB 1747539)

Current address: 104 TW Alexander Dr. Building 1, Research Triangle, NC 27709

Author for contact: Ben F. Holt III, bholt@agbiome.com

Abstract

Transcription factors (TFs) are fundamental components of biological regulation, facilitating the basal and differential gene expression necessary for life. TFs exert transcriptional regulation through interactions with both DNA and other TFs, ultimately influencing the action of RNA polymerase at a genomic locus. Current approaches are proficient at identification of binding site requirements for individual TFs, but few methods have been adapted to study oligomeric TF complexes. Further, many approaches that have been turned toward understanding DNA binding of TF complexes, such as electrophoretic mobility shift assays, require protein purification steps that can be burdensome or scope-limiting when considering more exhaustive experimental design. In order to address these shortfalls and to facilitate a more streamlined approach to understanding DNA binding by TF complexes, we developed the DIMR (**D**ynamic, **I**nterdependent TF binding **M**olecular **R**eporter) system, a modular, yeast-based synthetic transcriptional activity reporter. As a proof of concept, we focused on the NUCLEAR

55 FACTOR-Y (NF-Y) family of obligate heterotrimeric TFs in *Arabidopsis thaliana*. The
56 DIMR system was able to reproduce the strict DNA-binding requirements of an
57 experimentally validated NF-Y^{A2/B2/C3} complex with high fidelity, including recapitulation of
58 previously characterized mutations in subunits that either break NF-Y complex
59 interactions or are directly involved in DNA binding. The DIMR system is a novel,
60 powerful, and easy-to-use approach to address questions regarding the binding of
61 oligomeric TFs to DNA.
62

63 Introduction

64 Transcription factors (TFs) are a fundamental component of biological control, facilitating
65 differential gene expression in response to environmental stimuli and making complex life
66 possible. The mechanism through which differential gene expression manifests is
67 inherently complex, requiring coordination of stimulus perception, transcriptional and
68 translational responses, and alteration of relevant protein activity (Crick 1970). The
69 transcription-level integration of stimuli is of particular interest, as this process supports
70 context-specific recruitment of RNA polymerase to a specific genomic locus (Diamond et
71 al. 1990). This integration is accomplished through the independent, competitive, and
72 cooperative functions of TFs and the effects of these relationships on DNA-binding and
73 RNA polymerase recruitment (Amoutzias et al. 2008; Lickwar et al. 2012). A better
74 understanding of the mechanisms through which transcriptional activity are modulated,
75 particularly how TF interactions influence regulatory capacity, could facilitate the design
76 of more precise and predictable molecular tools to address long-standing issues in the
77 fields of agriculture, health care, and manufacturing, among others (Khalil and Collins
78 2010).

79
80 Current approaches to identify TF-DNA interactions are effective at *de novo* identification
81 of binding site preferences of individual TFs *in vitro* and at identifying global binding
82 patterns of individual TFs *in vivo*. In many cases, a combination of approaches can be
83 used for a more complete understanding of TF targeting. In particular, many researchers
84 have found great success in combining approaches that effectively identify binding
85 specificity (such as Protein Binding Microarrays (PBMs), 1-Hybrid-based library
86 screening, or DNA Affinity Purification (DAP-seq)) and lower-resolution, global-scale
87 binding site identification (such as Chromatin Immunoprecipitation (ChIP-seq) or Assay
88 for Transposase-Accessible Chromatin (ATAC-seq)).

89
90 While we will not focus on the general strengths of each approach or combination of
91 approaches (see reviews, (Mahony and Pugh 2015; Jayaram et al. 2016)), one aspect of
92 TF function that remains less explored is the impact that TF oligomerization exerts on
93 DNA binding (Jolma et al. 2015). Most approaches, including those introduced above,

94 have focused on understanding some aspect of DNA-binding of an assumed individual
95 TF; however, a much more complex interplay of TF function exists than can be readily
96 and methodically addressed with current techniques. Transcriptional regulation through
97 multi-component TF complexes is a common theme, but our understanding of how these
98 complexes identify and interact with specific genomic loci remains less explored (Jolma
99 et al. 2015; Morgunova and Taipale 2017). For example, a recent study identified
100 dramatic shifts in cognate binding sequences of bZIP homodimers compared to
101 heterodimers (Rodriguez-Martinez et al. 2017); however, the experimental approach
102 used in this study required purification of a large suite of individual transcription factors.
103 An approach enabling rapid and straight-forward testing of complex TF units, with the
104 ability to make targeted mutations in any component of the TF complex or its potential
105 binding site, would create a new lens through which we could explore more nuanced
106 aspects of TF-DNA interactions.

107
108 Traditional definitions of transcription factors often highlight the presence of both a DNA-
109 binding and a transcriptional-regulation domain; however, many TFs function as obligate
110 protein complexes, where individual components contain partial DNA-binding or
111 transcriptional-regulation domains that are only fully-reconstituted within the context of a
112 functional complex. One example of such an arrangement can be found in the NUCLEAR
113 FACTOR-Y (NF-Y) transcription factors, a complex that functions as an obligate hetero-
114 trimer of three distinct subunits, NF-YA, NF-YB, and NF-YC, and physically interacts with
115 the DNA sequence *CCAAT*. Although this complex was initially identified over 30 years
116 ago (Dorn et al. 1987; Jones et al. 1985), questions remain regarding the molecular forces
117 driving specificity of the NF-Y complex to *CCAAT*. Several key observations and studies
118 have led to persistent interest in the NF-Y, particularly in plant lineages, including: (1) the
119 ubiquitous nature of the *CCAAT* box and, subsequently, NF-Y regulated genes, (2) the
120 expansion of the NF-Y subunit families in plants compared to animals, where animals
121 encode 1-2 members of each subunit, while higher plants often encode 10+ of each
122 subunit (Siefers et al. 2009), and (3) the identification and molecular characterization of
123 the first non-canonical NF-Y complex in plants, which replaces an NF-YA subunit for a

124 plant-specific CCT (CONSTANS, CONSTANS-LIKE, and IOC1) domain-containing
125 protein, leading to altered DNA binding properties (Gnesutta et al. 2017).

126
127 Published crystal structures of various NF-Y complexes, particularly of the full *Homo*
128 *sapiens* NF-Y complex bound to DNA (Nardini et al. 2013), have raised increasingly
129 complex questions regarding the specificity of the NF-Y complex for a particular *CCAAT*
130 box. While all three NF-Y subunits have been shown to make physical contact with DNA,
131 it appears that only NF-YA makes sequence-specific contact, inserting directly into the
132 minor groove of the *CCAAT* box, while NF-YB and NF-YC make contacts with the DNA
133 backbone, appropriately positioning both the DNA and NF-YA subunit for tight physical
134 interaction (Nardini et al. 2013). Despite this understanding, the NF-Y complex appears
135 to show more selectivity than has been experimentally derived. For example, most
136 *CCAAT* boxes in human cell lines are not consistently bound by NF-Y complexes (Encode
137 Project Consortium et al. 2007; Zambelli and Pavesi 2017), meaning that the mere
138 presence of a *CCAAT* box is not predictive of NF-Y binding. Factors such as chromatin
139 accessibility and repressive epigenetic modifications regularly limit the binding landscape
140 of a given TF (John et al. 2011); however, the NF-Y are thought to function as ‘pioneer’
141 TFs that are able to bind less-accessible DNA and promote further TF complex formation
142 (Tao et al. 2017; Oldfield et al. 2014; Donati et al. 2008). Alternatively, while the only strict
143 requirement on NF-Y binding is the presence of the pentanucleotide *CCAAT*, the flanking
144 nucleotides could serve as a fine-tuning mechanism for complex binding and stability.
145 Ultimately, the source of this *CCAAT* box selectivity is not well understood and is made
146 significantly more complex when considering the expanded family size and combinatorial
147 complexity of plant NF-Y subunits.

148
149 In particular, we hypothesized that different NF-YB/NF-YC dimers might contribute to
150 *CCAAT* box selectivity through interactions with the nucleotides flanking the *CCAAT*
151 pentamer; however, comparing all possible NF-YB/NF-YC combinations with even a
152 single NF-YA component would be a significant undertaking, with 100 possible
153 combinations in *Arabidopsis thaliana* (Petroni et al. 2012) and 208 possible combinations
154 in *Oryza sativa* (rice, (Hwang et al. 2016)). *In vitro* approaches requiring protein

155 purification, such as Electrophoretic Mobility Shift Assay (EMSA), become time- and cost-
156 prohibitive at this scale. More importantly, many proteins are recalcitrant to protein
157 purification, and can only be isolated if appropriately truncated or co-expressed with other
158 factors. Despite these technical limitations, EMSA analysis is well-suited for these types
159 of investigations, and any approach intended to address similar questions would need to
160 match or complement its capabilities. A reporter system with a large dynamic range and
161 high sensitivity would allow scientists to address mutations that have much more modest
162 effects on TF-DNA interactions, and could facilitate examination of more precise or
163 biologically-relevant questions.

164

165 To address these issues and to better facilitate these types of research, we designed the
166 DIMR (**D**ynamic, **I**nterdependent TF binding **M**olecular **R**eporter) system (Figure 1), a
167 modular yeast-based transcriptional activity reporter system developed through repeated
168 application of the synthetic biology approach of build-test-learn. The DIMR system allows
169 for dose-dependent induction of a suite of transcription factors (effectors) and subsequent
170 monitoring of transcriptional regulation. We validated our approach by testing the DNA
171 binding and transcriptional activation capabilities of the Arabidopsis NF-Y^{A2/B2/C3} complex
172 and found that the DIMR system was able to faithfully recapitulate both wild-type CCAAT
173 box binding and previously-described mutations impacting DNA binding and complex
174 formation.

175

176 **Results**

177 *DIMR system components, design philosophy, and functional description*

178 The DIMR system is composed of three modules: (1) an **Activator Module**, encoding an
179 inducible artificial transcription factor (ATF), (2) an **Effector Module**, encoding a single
180 ATF-driven cassette containing viral 2A 'cleavage' sites between effector components,
181 and (3) a **Reporter Module**, containing a dual-luciferase reporter composed of a
182 constitutively transcribed *Renilla* luciferase and a conditionally transcribed Firefly
183 luciferase (Figure 1A). Each module is carried on a yeast shuttle vector with different
184 auxotrophic selection, and each has been designed to be as modular as possible, with
185 restriction enzyme sites strategically placed to facilitate swapping individual effector or

186 reporter components with minimal laboratory effort. As currently implemented, point
187 mutations in existing effectors can be easily accomplished through commercially available
188 site-directed mutagenesis kits, novel effector modules can be synthesized *de novo* at
189 affordable rates, and permutations of binding sites can be cloned in as little as 3 days at
190 a relatively low cost and with very minimal active time, resulting in a streamlined, quick,
191 and hands-off assay to investigate TF-DNA interactions (Figure 1B). Finally, because of
192 the synthetic biology-based approach taken during the design and implementation of the
193 system, each component of the modules can easily be further iterated upon for improved
194 function or to accomplish different goals.

195
196 The Activator module (Figure S1) utilizes the chimeric Z₄EV artificial transcription factor,
197 which contains three functional domains: (1) an engineered zinc finger with specificity to
198 a DNA sequence not found in the genome of *Saccharomyces cerevisiae*, (2) an estrogen
199 receptor that modulates activity and localization, and (3) a VP16 activation domain
200 (McIsaac et al. 2013). Z₄EV is constitutively expressed under the *ACT1* promoter
201 (Flagfeldt et al. 2009) but remains inactive and restricted to the cytosol. Activation of Z₄EV
202 with the hormone β -estradiol initiates translocation to the nucleus and activation of the
203 Effector cassette. This activation was previously shown through transcriptome profiling to
204 induce remarkably few unintended effects, either through the action of β -estradiol itself or
205 through off-target binding of Z₄EV (McIsaac et al. 2013).

206
207 The Effector module (Figure S2) is designed to emulate a polycistronic message through
208 the incorporation of viral 2A 'self-cleaving' sequences. Our initial designs included
209 cassettes expressing both 2 and 3 genes, with a translationally-fused flexible linker and
210 unique epitope tag on each (Sabourin et al. 2007). The linkers between components A –
211 B and B – C also encode previously-validated T2A peptide sequences (Beekwilder et al.
212 2014), facilitating translation of individual proteins from a single mRNA. Restriction
213 enzyme recognition sites were embedded into the coding sequences of the T2A linkers
214 through the introduction of silent mutations. This allows easy swapping of effectors
215 through either (1) the inclusion of the appropriate flanking linker sequence through gene

216 synthesis (recommended, along with codon optimization (Kotula and Curtis 1991;
217 Gustafsson et al. 2004)) or (2) PCR amplification to produce the appropriate over-hangs.

218
219 The Reporter module (Figure S3) encodes a dual luciferase reporter system, including a
220 *Renilla* luciferase variant constitutively expressed under the *ACT1* promoter, and a
221 conditionally expressed Firefly luciferase variant. Design of the Firefly luciferase promoter
222 drew heavily on previously characterized yeast promoters bound by yeast NF-Y
223 complexes. Specifically, we chose native, experimentally validated promoters of
224 *Saccharomyces cerevisiae* whose activation required the presence of a specific *CCAAT*
225 box (implying direct regulation by the NF-Y), and replaced the required *CCAAT* box
226 binding site with the various permutations described below. Cloning of binding site
227 permutations is quick and simple, requiring only a pair of appropriately designed, 5'-
228 phosphorylated oligonucleotides and simple restriction enzyme digestion and ligation
229 reactions.

230

231 *Validation of effector induction and cleavage*

232 As a starting point, we tested our ability to induce accumulation of Arabidopsis NF-
233 Y^{A2/B2/C3} effectors through the activation of Z₄EV. After a 6-hour induction period, we were
234 able to visualize accumulation of NF-YA2:HA (Figure 2A), NF-YB2:MYC (Figure 2B), and
235 NF-YC3:FLAG (Figure 2C). Differences were seen in the level of protein accumulation
236 across samples, and several instances of failed T2A-mediated cleavage were clear;
237 however, we were able to clearly and consistently observe individual NF-Y subunits in
238 repeated experiments.

239

240 Further experiments to explore the inducibility of the effector cassette identified detectable
241 levels of individual effector proteins with around 5 nM β -estradiol (Figure S4), with no
242 obvious differences in accumulation between the different NF-Y subunits. A short time-
243 course of effector accumulation at 10 nM β -estradiol identified fairly stable accumulation
244 of individual effector proteins at 3 and 6 hours, though we often observed a peak
245 accumulation at 6 hours and a drop-off in signal when extending to 9 hours (Figure S5).
246 From these and other preliminary data, we established standard low- and high-induction

247 ranges of ~1 nM and ~10 nM β -estradiol, respectively, and a standard induction length
248 of 6 hours. While incomplete cleavage of individual effectors remains to be addressed,
249 the induction scheme of the DIMR system is effective and robust.

250

251 Validation of reporter activity following effector induction

252 Our initial system design and testing were built upon a previously-characterized NF-Y
253 regulated CCAAT box from the *FLOWERING LOCUS T (FT)* promoter in Arabidopsis.
254 This CCAAT box, as well as 20 flanking base pairs upstream and downstream, was
255 positioned immediately upstream of the minimal NF-Y regulated yeast promoter of
256 *CITRATE SYNTHASE1 (CIT1)*. Upon induction of the NF-Y^{A2/B2/C3} effector cassette, we
257 observed a significant, dose-dependent increase in relative luminescence (Figure 3A).
258 Normalization of the data into a fold change value, relative to mock induction, found an
259 average ~3.5-fold increase in high induction conditions (10 nM, Figure 3B). Despite the
260 successful recapitulation of NF-Y DNA binding in our initial designs, we were not able to
261 statistically distinguish between low- and high-induction conditions, and the maximum fold
262 changes observed were lower than desired. A larger dynamic range of reporter activation
263 would facilitate addressing more nuanced questions, such as the DNA binding impact of
264 individual effector mutations or changes in cognate binding sites.

265

266 Refinement of binding site design

267 From these initial tests, we next sought to refine the DIMR system for increased reporter
268 dynamic range. We focused our system tuning on two approaches: reducing mock-level
269 signal and increasing maximum activation. To decrease mock-level signal, we designed
270 and tested different NF-Y regulated minimal promoter architectures to identify reporters
271 with lower basal level activation. We focused on promoters for the genes *CIT1* and
272 *ASPARAGINE SYNTHETASE1 (ASN1)*, driven by the above-described *FT* CCAAT box
273 footprint (Figure 4A). Luciferase activity levels were lower in mock-treated samples with
274 the *ASN1*-based promoter compared to the originally-tested *CIT1*-based promoter
275 (Figure 4B). Notably, this reduction in mock-level activation translated to a larger fold
276 change of ~6x in *ASN1*-based reporters when comparing mock and high induction
277 conditions.

278

279 To increase our maximum signal, we additionally tested the effects of different numbers
280 of binding sites and the spacing between them. Multimerization of available binding sites
281 can result in an increase in observed transcriptional activity (Khalil et al. 2012), but this
282 larger DNA footprint can be more difficult to accommodate in cloning. To abrogate this,
283 we also tested the effects of reducing the length of each individual binding site footprint.
284 First, we attempted to cut the *CCAAT* box footprint roughly in half by including only 10
285 base pairs of flanking sequences in single, double, and triple binding site configurations
286 (Figure 4C), and found that multimerization of the binding site increased total system
287 activation. Finally, we combined the original, larger *CCAAT* box footprint into single,
288 double, and quadruple binding site configurations (Figure 4D). In this set, the quadruple
289 binding site configuration stands out at a much-improved ~15-fold increase in reporter
290 activity from mock. The larger DNA footprint of the quadruple binding site approach
291 required a slightly modified cloning approach, where two pairs of annealed,
292 phosphorylated oligos were simultaneously ligated into the Reporter module; however,
293 we were able to preserve the flexibility of the DIMR system and avoided the need for
294 further gene synthesis for individual binding site permutations.

295

296 *Validation and assessment of refined binding site setup*

297 With an increased signal level upon system activation, we began testing the activation
298 requirements of the DIMR system. First, we examined dose-dependent system activation
299 levels of the NF-Y^{A2/B2/C3} complex on the quadruple *CCAAT* box over a wide range of β -
300 estradiol induction levels (Figure 5A). This induction gradient was analyzed through 4-
301 parameter logistic regression (4PLR), with an R^2 value of 0.942. No system activation
302 was observed at induction levels below 1 nM, while activation peaked between 10 and
303 100 nM β -estradiol. The dose-dependent activity of the system was most pronounced
304 between 1 nM and 10 nM, with a half maximal effective concentration (EC_{50}) of ~2.2 nM
305 and total span of ~10.5-fold change. 4PLR is a widely used metric in chemistry,
306 biochemistry, and computational biology to describe cooperative action, and in this case,
307 statistically supports the idea that the individual NF-Y subunits are working
308 interdependently in an induction-dependent manner to bind the *CCAAT* box.

309

310 To further solidify the correlation between effector induction and system activation, we
311 tested the impacts of loss of individual DIMR modules, previously described mutations in
312 NF-Y effectors, and changes in the CCAAT box (Figure 5B). Replacing either the Z₄EV
313 activator cassette or the NF-Y effector cassette with empty vectors resulted in a complete
314 loss of system activation upon induction. Importantly, we found that mutation of the
315 CCAAT box to CCAGC eliminated system activation. These three pieces of data
316 collectively suggest that the observed induction responses are accomplished through the
317 action of the NF-Y complex on the CCAAT box driving the firefly luciferase reporter.

318

319 We also performed further system tests with the *NF-YB2 E65R* point mutation, a
320 previously characterized mutation shown to prevent interaction of the NF-YB/NF-YC
321 dimer with NF-YA (Sinha et al. 1996; Siefers et al. 2009). As expected, this point mutation
322 abolished system activation (Figure 5B). While many highly-conserved residues in each
323 of the NF-Y subunits have been previously identified and characterized to completely
324 break DNA binding (Sinha et al. 1996; Kim et al. 1996; Sinha et al. 1995), we wanted to
325 examine novel mutations that could help reveal the evolutionary constraints acting on the
326 NF-Y complex. To this end, we examined the effects of one particular point mutation at a
327 residue thought to be directly involved in CCAAT box binding, *NF-YA2 H183A*. With the
328 native histidine residue replaced with an alanine at this location, we still observed a
329 moderate level of system activation (Figure 5B). This alanine-replacement approach is
330 traditionally used to replace residues that contribute to sequence-specificity with an
331 unobtrusive and relatively-inert alanine that is unlikely to mediate sequence-specific
332 interactions (Luscombe et al. 2001).

333

334 Because we had previously observed instances of failed 2A site function in the form of
335 fused effector components, we directly tested whether these fused effectors were
336 functional by creating point mutations that break the existing 2A sites. We found that
337 fusion of the NF-YA and NF-YB components did lower maximum reporter activity
338 compared to a 2A-cleaved trimeric system or a fusion between NF-YB and NF-YC, but
339 each instance of broken 2A cleavage was still able to significantly activate the reporter

340 system (Figure S6). While not all transcription factor complexes will be able to effectively
341 form and regulate DNA while fused together, this should be tested for each group of
342 transcription factors being tested.

343

344 Finally, we tested whether yeast NF-Y orthologs might be able to compete with or take
345 the place of our effector module-encoded Arabidopsis NF-Y proteins. Sequentially
346 removing one NF-Y subunit from the otherwise-complete effector module induced no
347 system activation (Figure S7), suggesting that native NF-Y orthologs are not responsible
348 for any significant activation of the reporter. While interactions between NF-Y orthologs
349 of different species has been demonstrated (Calvenzani et al. 2012), we hypothesized
350 that the level of induction through the activator and effector modules would quickly
351 saturate any unintended interactions. Further, not all yeast NF-Y orthologs are thought to
352 be constitutive expressed, with at least one ortholog only expressed in response to non-
353 fermentable carbon sources (Bourgarel et al. 1999).

354

355 Validation of CCAAT-based NF-Y binding

356 To further explore the affinity of the NF-Y complex to the CCAAT box, we tested
357 permutations of the CCAAT box with variation at the 3' end, corresponding to all possible
358 combinations of CCANN (Figure 6). We focused on variation at these locations because
359 the crystal structure of the DNA-bound human NF-Y complex identified many more direct
360 interactions with NF-YA and the first three bases of the CCAAT box than the fourth and
361 fifth bases. Beyond this, our earlier exploration of the NF-YA2 H183A mutation suggests
362 possible differences in the way human and plant NF-Y complexes bind DNA, an idea
363 further supported by key differences in the otherwise-conserved linker region of NF-YA2.
364 This linker region was proposed to be important for precise positioning of flanking α -
365 helices for proper NF-Y complex stabilization and DNA binding, and NF-YA2 is the only
366 family member in Arabidopsis with this unusually long linker region.

367

368 Unsurprisingly, the highest-activated binding site of the CCANN suite was CCAAT at ~14-
369 fold over mock, with no other binding site permutation activating greater than 2.2-fold over
370 mock (Figure 6A). Among these non-CCAAT binding sites, we saw a small increase in

371 reporter activity in *CCANT*, but not in *CCAAN* (Figure 6B). A targeted comparison of these
372 two binding site permutations identified significant increases relative to mock in all
373 *CCANT* binding sites, but none other than *CCAAT* in the *CCAAN* variants (Figure 6C).
374 While further investigation is necessary, this observation runs counter to what is currently
375 understood about DNA binding by the NF-Y complex in humans, as a direct physical
376 interaction between NF-YA has been identified at the fourth position, but not the fifth
377 position, of the *CCAAT* box.

378

379

380 **Discussion**

381 *Using DIMR to investigate TF complex-DNA interactions*

382 In spite of the importance and ubiquitous nature of multi-component transcription factor
383 assemblies, relatively few molecular or biochemical approaches have been devised to
384 explore the intricacies of DNA binding by these multimeric complexes. Current and widely
385 adopted methods are not well-suited for many questions, particularly those that could
386 benefit from extensive mutagenesis-based analyses, such as alanine scanning
387 mutagenesis to probe the relative contributions of DNA binding amino acids within a given
388 TF. After fine-tuning and optimizing our induction and binding site schemes, we ultimately
389 produced a sensitive, straightforward, and versatile reporter system for assaying
390 transcription factor complex DNA interactions. As one example of this type of study, we
391 examined the effect of permutations of the *CCAAT* box and identified a slightly higher
392 level of system activation when altering bases at position 4 than position 5 (*CCANT* vs.
393 *CCAAN*). Our system bypasses the need for protein purification or deep sequencing, two
394 common requirements for other approaches. The proposed system can easily be scaled
395 to simultaneously include dozens of effector or binding site permutations with relative
396 simplicity, and requires only relatively basic lab equipment. The injector-fitted,
397 luminescence-based plate reader is likely the only equipment not commonly found in a
398 standard molecular lab, and these types of equipment are often housed in core facilities
399 available to most universities or institutes.

400

401 *Incomplete cleavage at T2A sites in effector module*

402 Our initial designs sought to leverage viral 2A peptide sequences to generate equimolar
403 amounts of individual effectors through a cleavage mechanism during translation, an
404 important goal when considering obligate oligomeric TF complexes. We use the term
405 cleavage throughout; however, strictly speaking, the end result is an inability to form the
406 peptide bond between two adjacent amino acids, not true cleavage of an existing peptide
407 bond (Kim et al. 2011). Because eukaryotes do not utilize the polycistronic mRNA
408 approach so common in bacteria, researchers have turned to 2A sites and other
409 approaches to emulate this effect. While not a perfect solution to this problem, we found
410 that viral T2A sites worked sufficiently well for our needs here. It is important to note,
411 however, that incomplete cleavage of the effector cassette does alter the interpretation of
412 system activation. Therefore, with the shortcomings of this design, we can test whether a
413 transcription factor complex can bind *a particular consensus sequence*, but we cannot
414 directly address whether a particular complex *can or cannot form*. While this distinction is
415 fairly minor in many cases, particularly when working with previously-described
416 complexes, it is an important limitation of the system that should be addressed in future
417 iterations. Unfortunately, no completely effective eukaryotic-based system has been
418 described to recreate the polycistronic mRNA system so widely employed in bacteria
419 (Blount et al. 2012). However, new 2A peptide sequences are still being identified and
420 have been seen to vary in efficiency from organism to organism (Luke et al. 2010), raising
421 the possibility that a 2A site more efficient in yeast remains to be identified.

422

423 To circumvent this issue, we have begun designing effector cassettes with individual
424 components driven by separate inducible promoters. These separate promoters each
425 contain the Z4EV -bound consensus sequence, but utilize different minimal promoters to
426 reduce recombination within yeast (Broach et al. 1982). Whether this modification will
427 lead to relatively-equal protein accumulation is unknown; however, it should at least
428 provide a framework to begin further modifying, tweaking, and improving the system for
429 our specific needs.

430

431 *Considerations and improvements on the DIMR system*

432 While much of the parameter refinement presented above should help inform novel
433 design considerations, some applications will require more significant alterations. In
434 particular, issues are likely to arise where effector complexes do not possess intrinsic
435 transcriptional activation potential or when a binding site is bound and autoactivated by
436 endogenous yeast proteins. In cases where complexes completely lack activation
437 potential, an activation tag might be fused to one or more effectors (Knop et al. 1999);
438 however, whether this approach could overcome active transcriptional repression is
439 unclear. Similarly, instances of reporter autoactivation might be addressed through fusion
440 of one or more effector components to a transcriptional repressor domain (Edmondson
441 et al. 1996) and measuring inducible *reductions* of reporter activity. While we have not
442 yet worked through either of these concerns, the modular design of the system should
443 allow for relatively straight-forward modification and testing.

444

445 *Teasing apart the details of NF-Y DNA binding: a case for DIMR*

446 Despite consistent investigations into the mechanistic function of the NF-Y in animals
447 over the past 30 years, many aspects of complex formation and DNA binding remain
448 relatively unexplored in plant NF-Y orthologs. First, a significant amount of plant NF-Y
449 research, including most DNA-binding assays, has been conducted using only conserved
450 domains of each NF-Y subunit. In fact, the survey presented above represents one of the
451 first comprehensive examinations of DNA binding and transcriptional regulation by a
452 complete, full-length plant NF-Y trimeric complex. While the core domains of each NF-Y
453 subunit show significant conservation across all eukaryotic lineages, the flanking termini
454 show remarkable divergence from one another. The biological significance of these
455 flanking regions has remained elusive in most cases, though several protein-protein
456 interactions with NF-Y complexes are thought to be mediated through NF-Y terminal
457 domains (Cao et al. 2011). A better understanding of the functions of the less-conserved
458 termini is critical for plant NF-Y research in particular, as the vast majority of differences
459 between individual members of expanded NF-Y gene families are found in these flanking
460 regions. The DIMR system is capable of facilitating a systematic domain-swap approach
461 of the flanking regions of NF-YB or NF-YC paralogs, and could potentially uncover

462 changes in NF-Y complex affinity or specificity achieved through modulation of the
463 specific NF-Y subunits within a functional complex.

464
465 Like *NF-YB* and *NF-YC*, the conserved domains of *NF-YA* family members are
466 remarkably similar to one another. One critical exception to this observation is a 4-5 amino
467 acid elongated linker sequence encoded in the *NF-YA2* subunit. This linker is positioned
468 between two highly-conserved alpha helices that are each responsible for NF-Y complex
469 formation or DNA binding of the mature complex, and in addition to influencing the
470 positions of the flanking alpha helices, this linker also makes physical contact in several
471 places with the sugar-phosphate backbone of the *CCAAT* box (Nardini et al. 2013; Romier
472 et al. 2003). While experimental evidence is necessary to understand the impact and
473 significance of this atypical linker, it is possible that NF-Y complexes containing NF-YA2
474 have slightly different DNA binding profiles or NF-Y complex dissociation constants. It
475 should be noted, however, that NF-YA2 is likely the best-characterized plant NF-YA
476 subunit, as it has been a major focus of research through its regulation of photoperiodic
477 flowering. While the majority of our observations regarding NF-YA2 DNA binding and
478 complex formation have supported the crystal structure of the DNA-bound human NF-Y
479 complex, many important aspects of NF-Y form and function have not been thoroughly
480 investigated and developed.

481
482 In fact, many of the most exciting and significant advances in NF-Y research have
483 occurred in the last two years through the identification and characterization of the first
484 non-canonical NF-Y complex. This complex utilizes the NF-YB2/NF-YC3 dimer to
485 stabilize interactions between CONSTANS (CO) and its consensus binding site. This
486 complex, termed NF-CO, recognizes a *CCACA* motif found in the proximal promoter of
487 the *FLOWERING LOCUS T (FT)* gene and is critical for proper photoperiodic floral
488 induction (Gnesutta et al. 2017). The interaction between CO and the NF-YB/NF-YC
489 dimer is mediated through a conserved, plant-specific CCT (**C**ONSTANS, **C**ONSTANS-
490 *LIKE*, and **I**OC1) domain that is found in over 40 genes in Arabidopsis (Griffiths et al.
491 2003; Farré and Liu 2013), raising the possibility of a significantly-expanded pool of
492 potential NF-Y or NF-CCT complexes. Excitingly, several families of CCT domain

493 containing proteins have been extensively studied and shown to be of critical importance
494 for photoperiodic flowering (Griffiths et al. 2003), circadian clock entrainment and
495 maintenance (Mizuno 2004), and seedling environmental responses (Reyes et al. 2004).
496 Unfortunately, testing hypotheses concerned with these non-canonical NF-CCT
497 complexes is far from straightforward, with over a decade passing between the initial
498 suggestions that CO might function through NF-YB/NF-YC to a complete set of work
499 describing the NF-CO complex. Systematic testing of the ability of different NF-CCT
500 complex to form and bind DNA is a massive undertaking, with over 4,000 possible NF-
501 CCT complexes to test. Further, while the two are clearly related, the CCT domain shows
502 key differences from the DNA-binding domain of NF-YA, and variation within CCT
503 members occurs at residues predicted to be important for DNA binding in aligned NF-YA
504 sequences. A systematic mutational analysis focusing on the differences between
505 important residues of aligned NF-YA and CCT members could create a map of critical
506 DNA-binding residues, and inform the search for cognate binding sequences of various
507 NF-CCT complexes.

508
509 The DIMR system is well-suited to address these types of questions on structure and
510 function, as supported by our analysis of the *NF-YA2 H183A* point mutation and our
511 comparison of NF-Y^{A2/B2/C3} system activation in *CCANT* and *CCAAN* permutations. The
512 *NF-YA2* histidine residue at position 183 is thought to make sequence-specific contact
513 with the *CCAAT* box (Gnesutta et al. 2017), but reduced DIMR system activation is still
514 observed in the *H183A* point mutation. Importantly, when aligning NF-YA and CCT DNA
515 binding domains, this residue diverges between, but not among, many clades and sub-
516 clades. Considering this pattern of divergence, it is intriguing to consider that this
517 particular residue might contribute to DNA binding specificity of different NF-CCT
518 complexes. The identification of an NF-YA mutation at this residue that retains some
519 activity could be relevant to this observation in an evolutionary context, as a sub-optimal
520 variant is thought to facilitate further functionalization by providing a novel evolutionary
521 trajectory (i.e., without such a permissive intermediate, purifying selection cannot be
522 overcome to reach a different high-fitness state (Poelwijk et al. 2007; Anderson et al.
523 2015)). Further, the relative tolerance of wild-type system activation at *CCANT* compared

524 to **CCAAN** is interesting to consider in light of the evolutionary constraints acting on the
525 functionalization of NF-Y and NF-CCT complexes. This permissiveness could provide
526 space for evolution to act, allowing suboptimal interactions to lead to novel functions of
527 the complex. Direct testing of these types of evolutionarily significant hypotheses is
528 technically challenging, requiring more exhaustive mutagenic approaches such as
529 alanine scanning mutagenesis and subsequent functional validation (Cunningham and
530 Wells 1989). The DIMR system presented here was designed to bridge the gap in tools
531 necessary to more directly address these types of more nuanced questions.

532

533 **Acknowledgements**

534 The authors would like to thank Dr. Scott Russell for assistance with grant administration.
535 Additionally, we thank Dr. Daniel Jones, Dr. Marielle Hoefnagels, Dr. Laura Bartley, and
536 Andrew Willoughby for their insightful and constructive comments on the preparation of
537 this manuscript. Finally, we thank the National Science Foundation for funding this
538 research through MCB EAGER 1747539.

539

540

541 **Methods**

542 ***Yeast strain selection***

543 The tests presented here all utilized the BY4735 (ATCC 200897) strain (*MAT α*
544 *ade2 Δ ::hisG his3 Δ 200 leu2 Δ 0 met15 Δ 0 trp1 Δ 63 ura3 Δ 0*), a derivation of the S288C
545 laboratory strain. BY4735 was obtained and is available from the American Type Culture
546 Collection (<https://www.atcc.org/>).

547

548 ***Yeast growth, transformation, and induction conditions***

549 Yeast strains were uniformly grown at 30C. Wild type strains were grown with constant
550 agitation in YAPD liquid medium and transformed through the traditional lithium-acetate
551 based approach, as previously described. Transformants were selected after 2-3 days
552 growth on synthetic medium lacking Leucine, Tryptophan, and Uracil (L⁻W⁻Ura⁻).

553

554 For DIMR system induction, colonies were first grown to saturation in liquid L⁻W⁻Ura⁻
555 media. Saturated cultures were then diluted 1:1 to a total sample volume of 500 μ L with
556 fresh liquid L⁻W⁻Ura⁻ media containing either ethanol (mock treatments) or one of a range
557 of β -estradiol concentrations. These 500 μ L induction samples were cultured on deep,
558 2mL 96-well plates for 6 hours before sample collection for dual luciferase reporter
559 testing. Plates were covered with Breathe Easy strips during induction.

560

561 Unless directly stated otherwise, each system test was conducted after 6 hours of
562 induction, with treatments corresponding to mock induction (ethanol only), low induction
563 (1-1.5nM β -estradiol), and high induction (10nM β -estradiol).

564

565 ***Module design and construction***

566 The individual modules were each incorporated and carried on a different yeast shuttle
567 vector – *pRS314* and *pRS315* for the effector and activator constructs, respectively, and
568 a modified *pRSII316* removing an *NcoI* recognition site within the *URA3* coding sequence
569 through site directed mutagenesis (described below) for the reporter construct. Initial
570 module designs were synthesized by Biomatik[®], while individual effector drop-in
571 components were synthesized by Genewiz[®].

572

573 The activator module encodes the Z₄EV artificial transcription factor, driven by the
574 constitutive *ACT1* promoter (Flagfeldt et al. 2009) and flanked by the *CYC1b* terminator
575 (Curran et al. 2013). The effector module uses the Z₄EV-bound promoter to drive
576 expression of the ‘polycistronic’ effector mRNA. Each component has been translationally
577 fused to a 5x-glycine flexible linker (Sabourin et al. 2007) and a unique epitope tag
578 (component A: HA, component B: MYC, component C: FLAG). Viral T2A sites were
579 incorporated after the HA and MYC tags to facilitate cleavage into individual effector
580 components. The entire cassette is flanked by the *CYC1b* terminator. The reporter
581 module situates the two luciferase variants in a tail-to-tail fashion. The constitutively-
582 active Renilla luciferase is expressed under the *ADH1* promoter (McIsaac et al. 2013)
583 and is flanked by the *ADH1* terminator (Curran et al. 2013), while the conditionally-
584 expressed Firefly luciferase is driven by a modified yeast minimal promoter (*ASN1* and
585 *CIT1* presented here, (Sundseth et al. 1997; Nevoigt et al. 2006)) that includes previously

586 described NF-Y bound CCAAT box sequences (Cao et al. 2014; Gnesutta et al. 2017;
587 Siriwardana et al. 2016) and is flanked by the CYC1b terminator. All plasmids used in this
588 study are freely available, and are described in Table S1.

589

590 ***Binding site and promoter architecture cloning, site directed mutagenesis***

591 Drop-in Binding Site (DIBS) cloning was accomplished through annealing of 5'
592 phosphorylated oligos and subsequent ligation into the reporter module. DIBS primers
593 were designed and ordered as pairs of complementary oligos that were then annealed
594 together by boiling for 5 minutes in annealing buffer (10mM Tris HCl, pH 8.0, 1mM EDTA,
595 50mM NaCl) and slowly cooling to room temperature. The reporter module was restriction
596 enzyme digested (SacI/BamHI, New England Biolabs) and dephosphorylated (Quick
597 Dephosphorylation Kit, New England Biolabs), then purified and concentrated through the
598 Zymo DNA Clean and Concentrator kit (PN). Ligations were set up with 3:1 ratios of
599 insert:backbone free ends with ~50-150ng of purified backbone.

600

601 Site directed mutagenesis was conducted on effector entry clones through New England
602 Biolabs Q5[®] Site Directed Mutagenesis Kit, following manufacturer's instructions. Primers
603 for mutagenesis were designed with guidance of the NEBaseChanger[™] tool, and
604 mutagenesis was verified through restriction enzyme digestion (where appropriate) and
605 Sanger sequencing through the University of Oklahoma's Biology Core Molecular Lab.

606

607 ***Western blots***

608 Total yeast proteins were extracted using Y-PER[™] Yeast Protein Extraction Reagents
609 (Thermo Scientific, Cat no: 78991) following manufacturer's protocol. The protein
610 concentrations were measured using Pierce[™] BCA Protein Assay Kit (Thermo Scientific,
611 Cat no: 23225) following manufacturer's protocol, and was quantified on a Synergy HTX
612 Multi-Mode Reader (BioTeK, USA) at 562 nm wavelength. The protein concentrations
613 were calculated through generation of a BSA standard curve. A total of 3 µg of protein
614 was loaded to Mini-PROTEAN TGX Stain-Free Gels (10% gel, BIO-RAD). Proteins were
615 transferred to standard PVDF membranes through an OWL semi-dry transfer apparatus,
616 and the presence of NF-YA2:HA, NF-YB2:MYC, or NF-YC3:FLAG was probed with high
617 affinity anti-HA primary antibodies (Roche, catalog no. 11 867 423 001), anti-MYC
618 (Abcam, catalog no. ab9106), and anti-FLAG (Abcam, catalog no. F3165) followed by
619 rabbit anti-rat (Abcam, catalog no. ab6734), goat anti-rabbit (Abcam, catalog no.
620 ab205718), and goat anti-mouse (Abcam, catalog no. ab6789) HRP-conjugated
621 secondary antibodies, respectively. A Bio-Rad ChemiDoc XRS imaging system was used
622 for visualizing the protein blot after incubations with ECL plus reagent (GE Healthcare,
623 catalog no. RPN2132).

624

625 ***Dual luciferase assays***

626 Dual Luciferase assays were performed on the BioTek[®] Synergy[™] HTX multi-mode plate
627 reader fitted with dual reagent injectors, using the Illumination[™] Firefly & Renilla
628 Luciferase Enhanced Assay Kit (Goldbio[®], cat# I-920) per manufacturer instructions, with
629 the following alterations: (1) we used only 5µL of each culture, (2) samples were not spun
630 down and/or washed, and (3) we used half-volume injections of both luciferase buffers.
631 Our initial system tuning followed the manufacturer instructions more strictly, and we

632 could determine either no functional difference or minor improvements between
633 manufacturer instructions and our modified instructions (data not shown).

634

635 ***Statistical approaches***

636 Statistics were calculated through Graphpad Prism. One-way ANOVA on relative
637 luminescence values was used for comparisons of DIMR system activation to mock
638 levels. When denoting significance in fold change-based metrics, the relative
639 luminescence data was used for statistical analysis.

640

641 ***Figure and model construction***

642 Individual graphs were generated through Graphpad Prism, while full figures were
643 composed in Adobe Photoshop CC2018. The model in Figure 1A was constructed in
644 Inkscape, while the flowchart in Figure 1B was constructed through draw.io v10.4.5
645 (<https://draw.io/>).

646

647

Figures and Tables

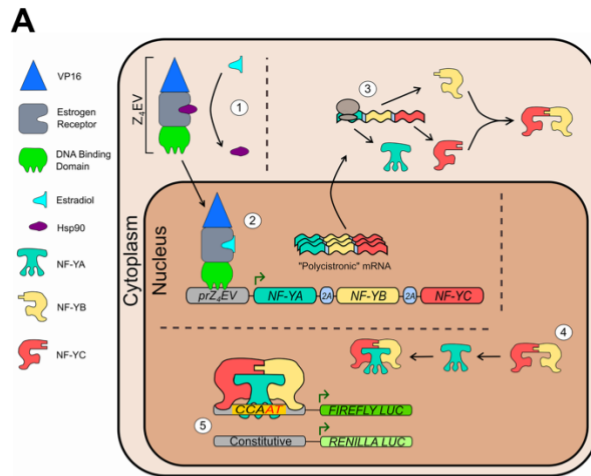
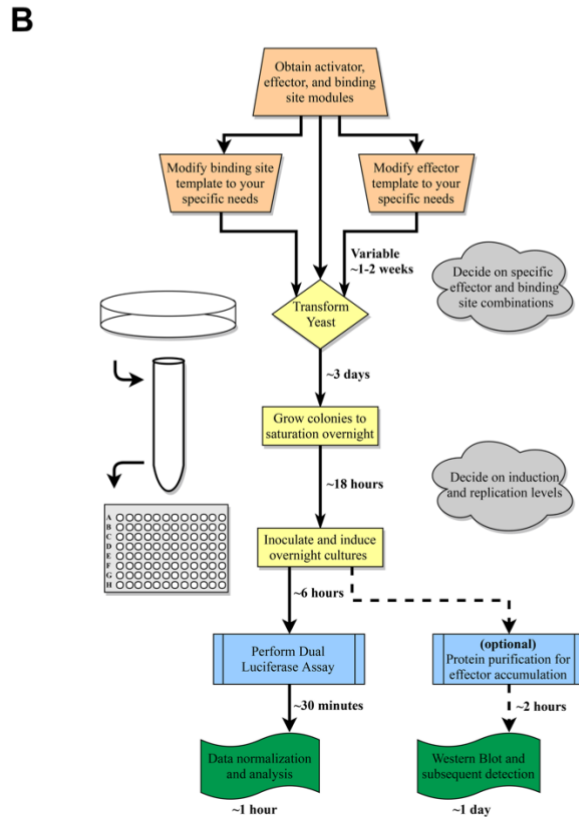


Figure 1. Model illustrating fundamental concepts and practical application of the DIMR system. (A) Circled numbers follow the flow of DIMR system activation: (1) β -estradiol activates the Z₄EV artificial transcription factor by competing with and replacing Hsp90, allowing for nuclear accumulation of Z₄EV; (2) Z₄EV induces transcription of the effector cassette; (3) translation of the effector cassette mRNA produces individual effector components through 2A-mediated translational cleavage; (4) effectors translocate to the nucleus and form functional complexes; and (5) transcriptional activation is measured as the ratio of conditionally-expressed firefly luciferase activity and constitutively-expressed Renilla luciferase activities from the reporter module. **(B)** Practical application of the DIMR system, including approximate timelines for design and implementation of an individual experiment.



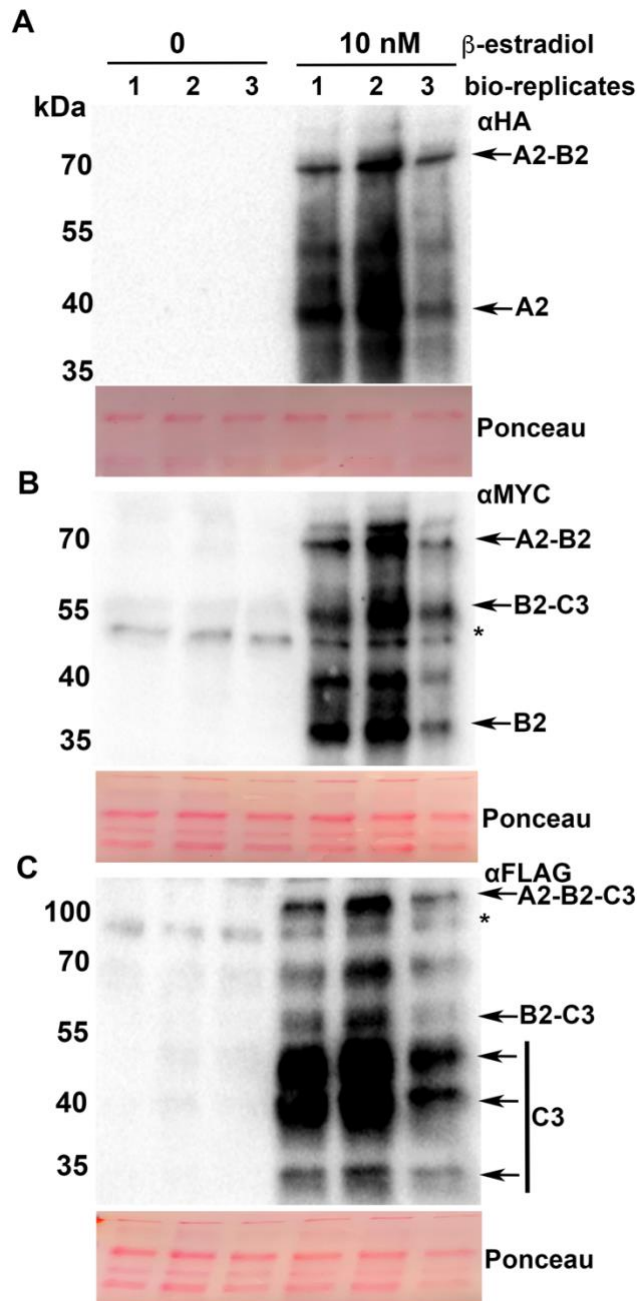
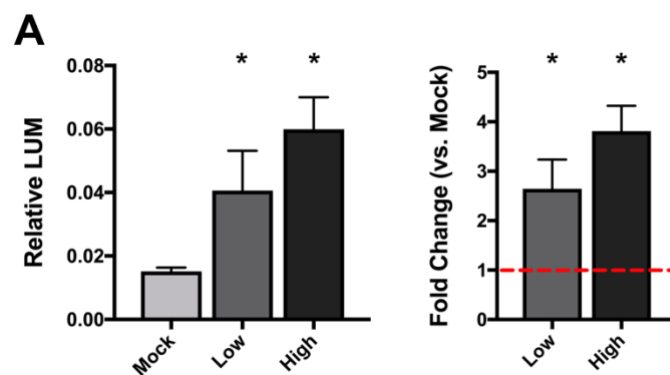


Figure 2. Induction and cleavage of NF-YA2, NF-YB2 and NF-YC3 effectors in yeast. Western blot analysis of **(A)** NF-YA2:HA, **(B)** NF-YB2:MYC, and **(C)** NF-YC3:FLAG accumulation in response to 10 nM β -estradiol induction for 6 hours. Three independent biological replicates, corresponding to lanes 1, 2, and 3, were tested for protein accumulation using anti-HA, anti-Myc and anti-Flag antibodies. Ponceau S staining of the PVDF membrane prior to transfer was used to test loading control. The experiment was repeated three times with similar result.



688
689 **Figure 3. DIMR system test of NF-YA2/B2/C3 on FT CCAAT box before system**
690 **optimization. (A)** Relative luminescence of mock, low, and high concentration β -estradiol
691 (0, 1uM, and 10uM, respectively) treated samples, and fold change levels (compared to
692 mock) of low and high treated samples. Each condition includes at least 6 biological
693 replicates. Asterisks indicate a significant increase between mock and treated samples,
694 as determined through two-way ANOVA ($p < 0.01$). Error bars represent 95% confidence
695 intervals.
696
697

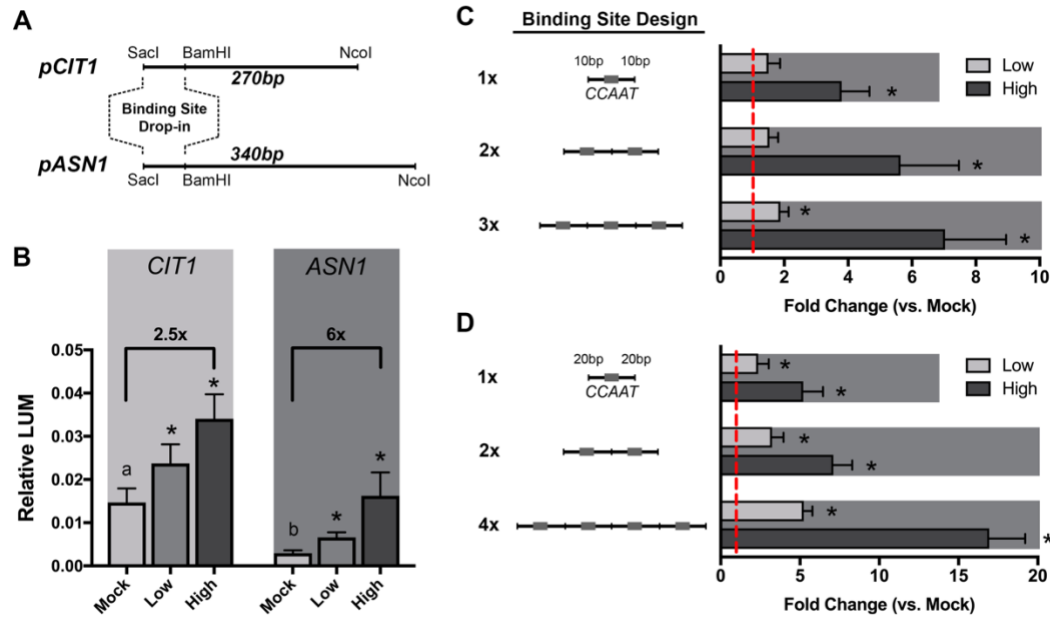


Figure 4.

698
 699 **Parameter refinement of the DIMR system to optimize reporter dynamic range. (A)**
 700 Model of two tested promoter architectures, derived from the *CIT1* and *ASN1* native yeast
 701 promoters. Binding site permutations were cloned into the reporter module through
 702 flanking *SacI* / *Bam*HI restriction sites. **(B)** Effects of different promoter architectures of
 703 *CIT1* and *ASN1* on DIMR system activation of NF- $\gamma^{A2/B2/C3}$ on *FT* CCAAT box. **(C, D)**
 704 Effects of binding site multimerization and altered spacing between binding sites. In **(C)**,
 705 each binding site footprint was 25bp, while in **(D)**, each footprint was 45bp. Both sets
 706 were testing binding of NF- $\gamma^{A2/B2/C3}$ on *FT* CCAAT box permutations in the *ASN1*-based
 707 promoter architecture. Error bars represent 95% confidence intervals. Asterisks above
 708 individual bars indicate statistical significance over matched mock-treated samples, as
 709 determined through two-way ANOVA ($p < 0.01$). Asterisks above brackets connecting two
 710 bars indicate significance between the two conditions, determined similarly. Letters above
 711 mock-induced bars indicate significance groups between the different promoter
 712 architectures, also determined through two-way ANOVA ($p < 0.01$).

713
 714

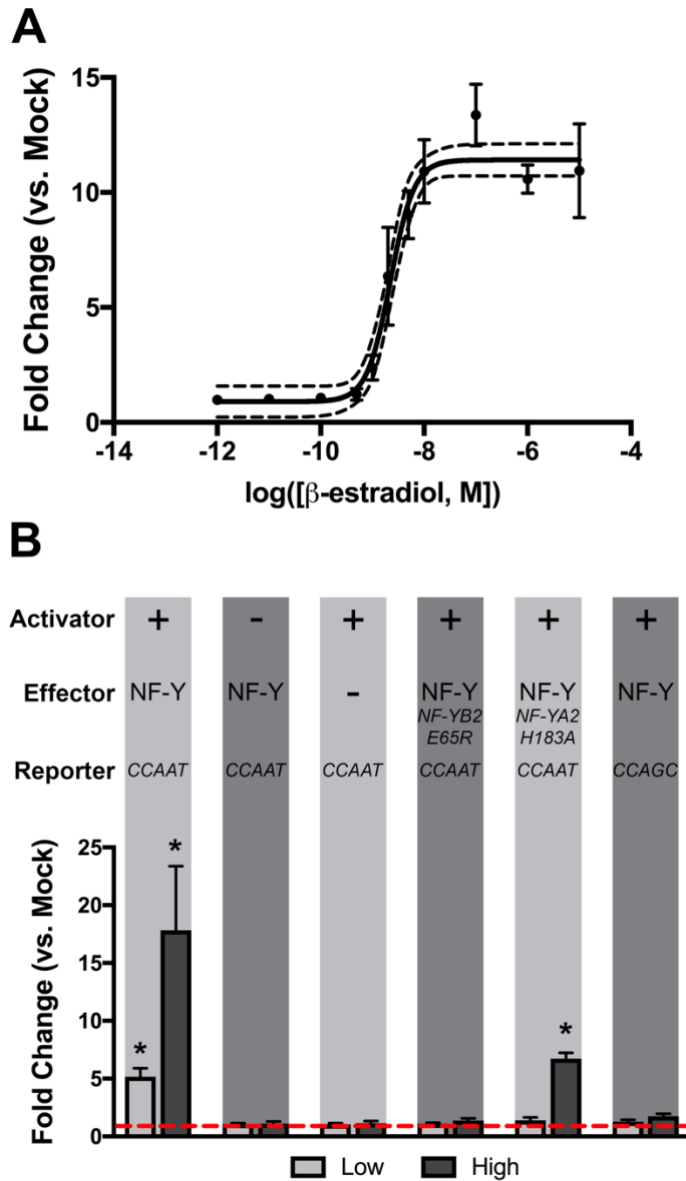
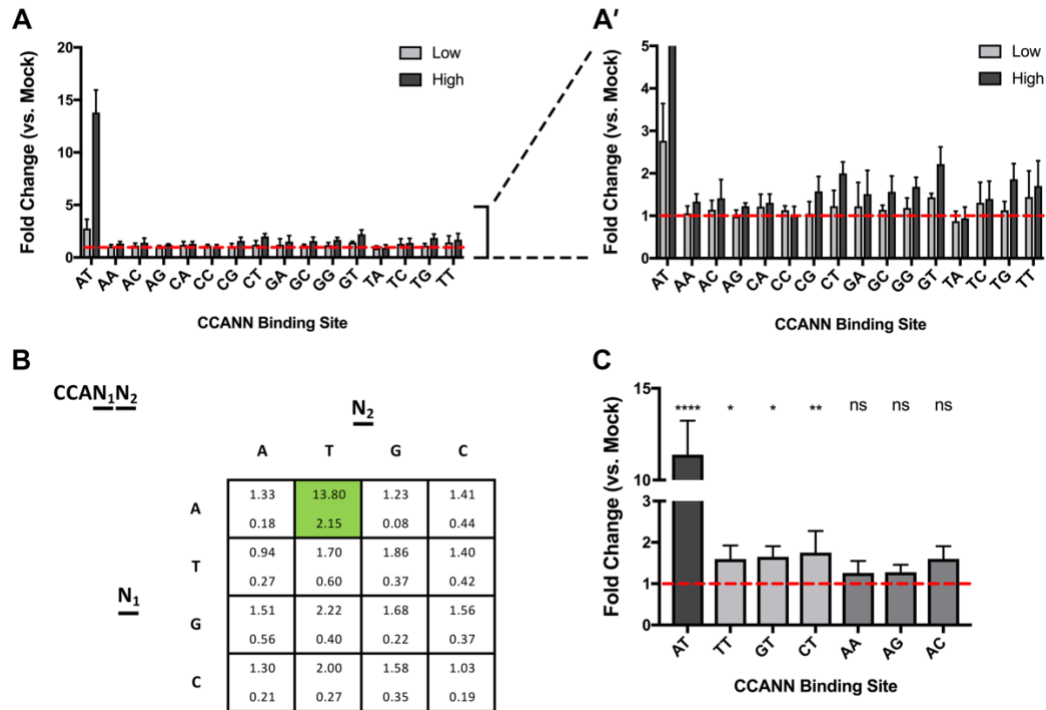


Figure 5. Functional assessment of DIMR system activation.

(A) Dose response curve of NF-Y^{A2/B2/C3} on the 4x *FT CCAAT* box in the *ASN1* promoter architecture. The solid line fits the dataset to a 4-parameter logistic regression, with 95% confidence intervals plotted with dashed lines ($R^2 = 0.942$). **(B)** DIMR system requirements for NF-Y/CCAAT-mediated activation. Module components are generally described above each condition: +, present; -, absent; NF-Y, NF-Y^{A2/B2/C3}. Error bars represent 95% confidence intervals. Asterisks above individual bars indicate statistical significance over matched mock-treated samples, as determined through two-way ANOVA ($p < 0.01$); all bars lacking asterisks were found to be nonsignificant compared to matched mock-treated samples.

741



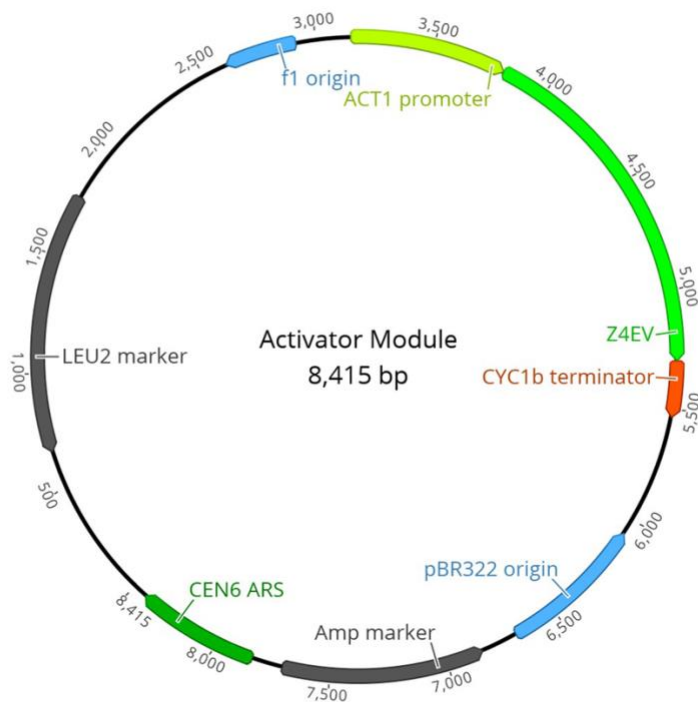
742

743

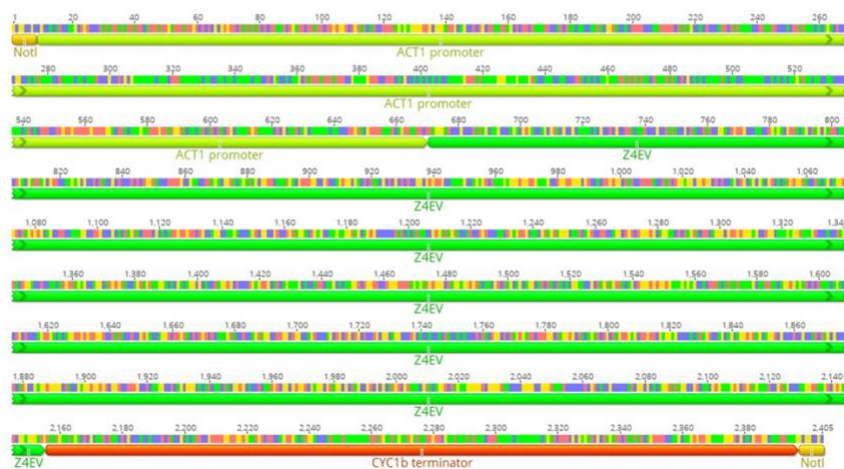
744 **Figure 6. DIMR-based validation and investigation of NF-YA2/B2/C3 CCAAT**
 745 **binding. (A)** System activation of NF-Y^{A2/B2/C3} on the *FT* CCAAT box, with all possible
 746 binding site permutations corresponding to CCANN. Error bars represent 95% confidence
 747 intervals. Asterisks above individual bars indicate statistical significance over matched
 748 mock-treated samples, as determined through two-way ANOVA ($p < 0.01$); all bars
 749 lacking asterisks were found to be nonsignificant compared to matched mock-treated
 750 samples. **(B)** Graphical representation of the data presented in panel A. Each cell
 751 corresponds to a specific permutation of CCANN, and contains the average fold change
 752 (top) and standard deviation (bottom). **(C)** A targeted comparison of CCANT and CCAAN
 753 binding site permutations. Asterisks indicate significance compared to mock induction as
 754 determined by two-way ANOVA with Sidak's multiple comparison adjustment (****, $p <$
 755 0.001 ; **, $p < 0.01$; *, $p < 0.05$).
 756

757

A



B



758

759

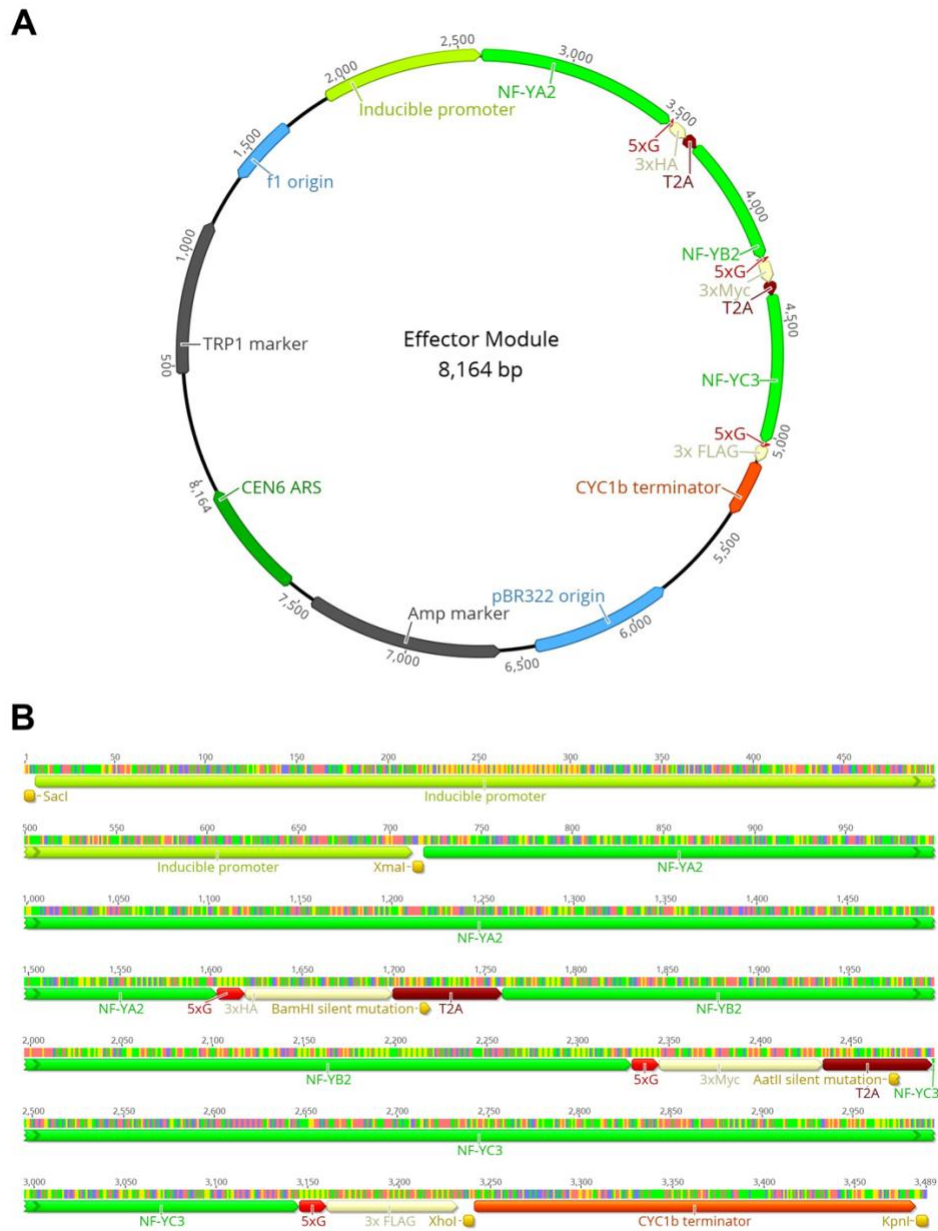
760

761

762

763

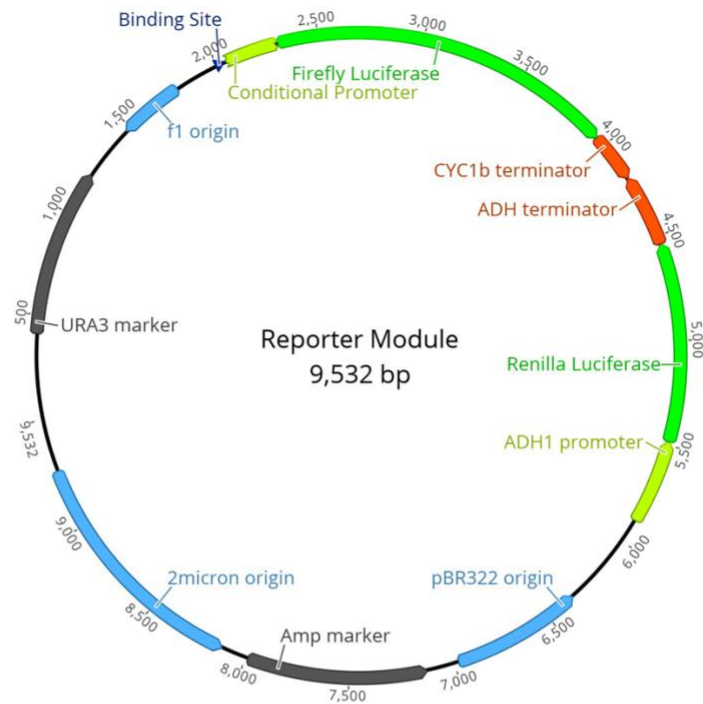
Figure S1. Main features of the Activator module. (A) Plasmid map of the DIMR Activator (pDIMR_A###) module showing important features and their orientation. (B) Zoomed-in view of the relevant Activator components.



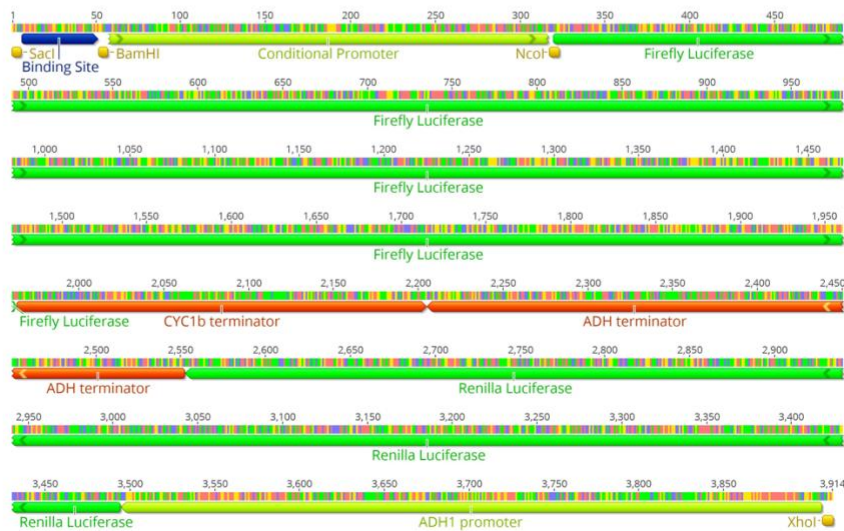
764
765 **Figure S2. Main features of the Effector module.** (A) Plasmid map of the DIMR Effector
766 (pDIMR_E###) module showing important features and their orientation. (B) Zoomed-in
767 view of the relevant Effector components, including important restriction enzymes used
768 for swapping new components into or out of the system.

769
770

A



B



771

772

773

774

775

Figure S3. Main features of the Reporter module. (A) Plasmid map of the DIMR Reporter (pDIMR_R###) module showing important features and their orientation. (B) Zoomed-in view of the relevant Reporter components, including important restriction enzymes used for Drop-In Binding Site (DIBS) cloning.

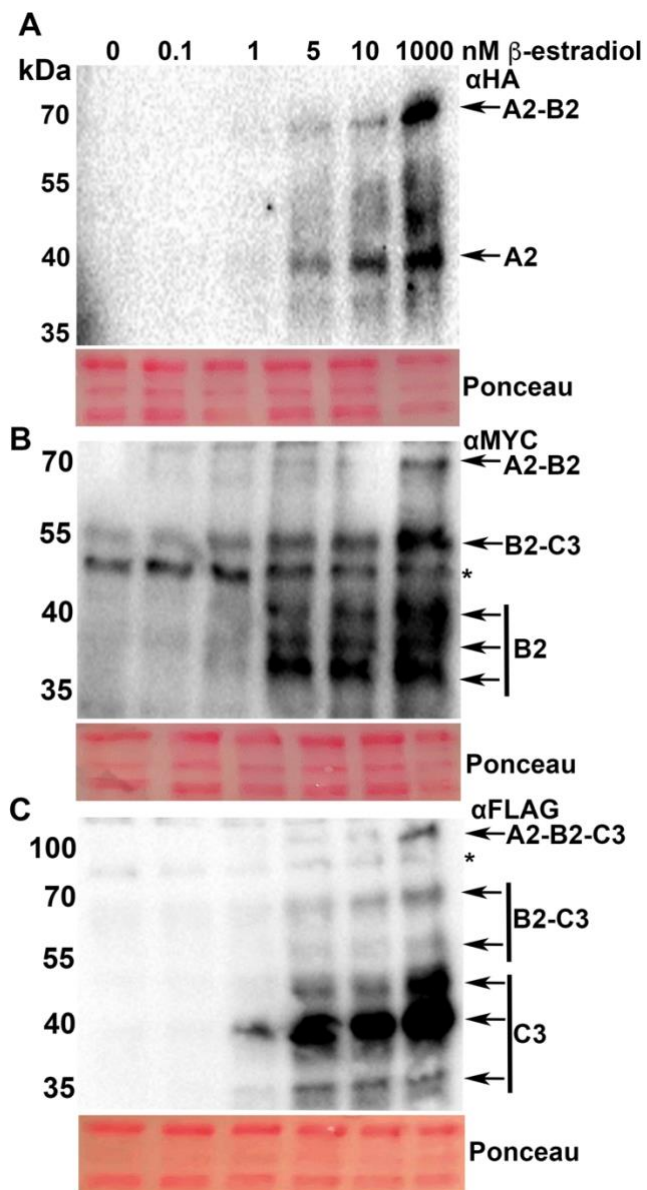


Figure S4. Induction gradient of NF-YA2, NF-YB2 and NF-YC3 effectors in yeast. Western blot analysis of (A) NF-YA2:HA, (B) NF-YB2:MYC, and (C) NF-YC3:FLAG accumulation in response to varying levels of β -estradiol induction for 6 hours. A single biological replicate was tested for protein accumulation using anti-HA, anti-Myc and anti-Flag antibodies. Ponceau S staining of the PVDF membrane prior to transfer was used to test loading control. The experiment was repeated twice with similar results.

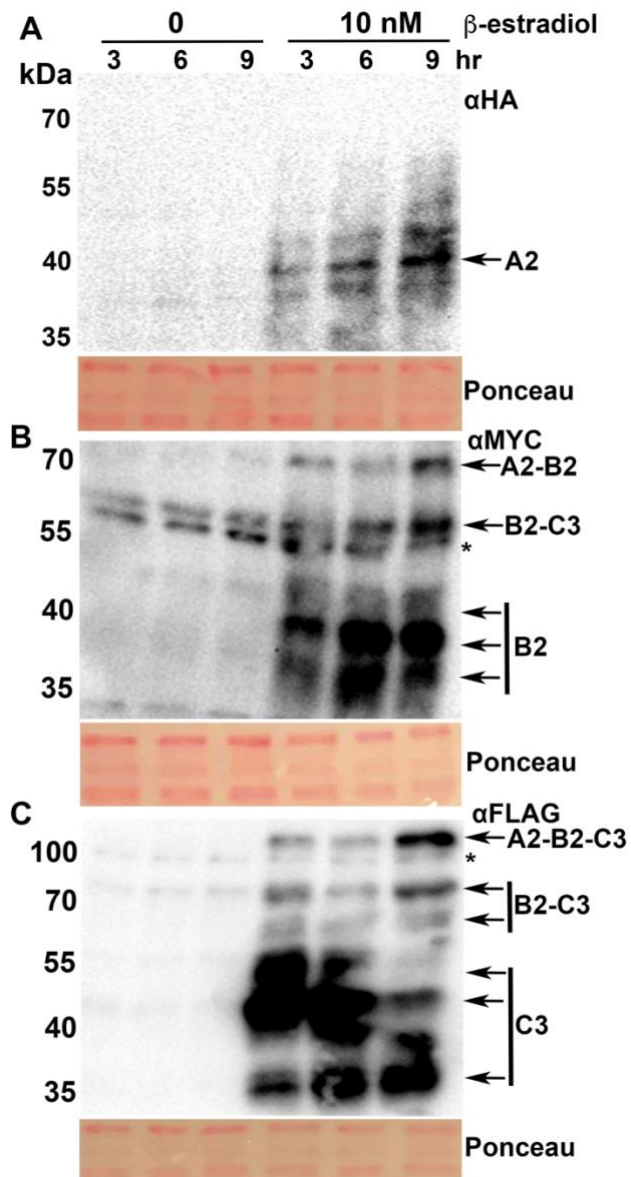
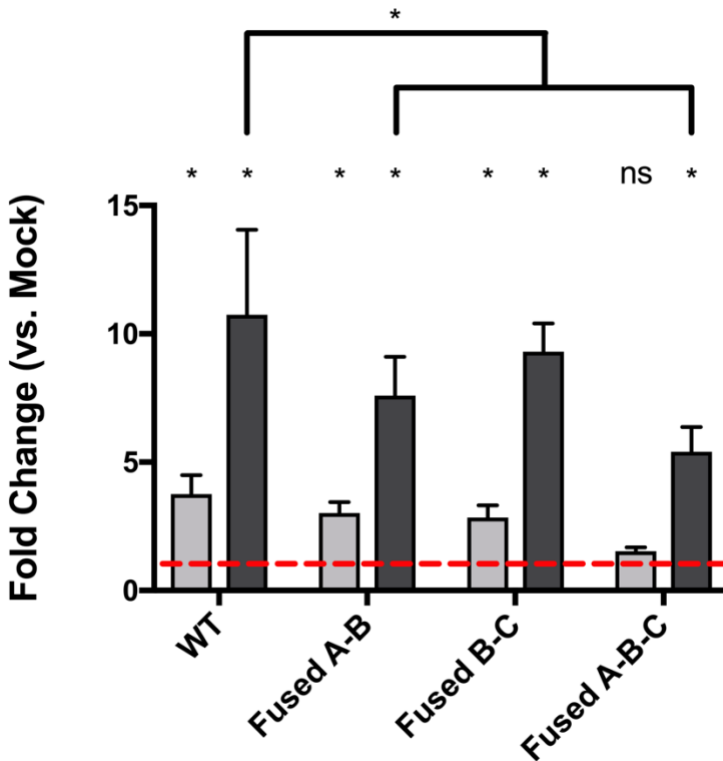
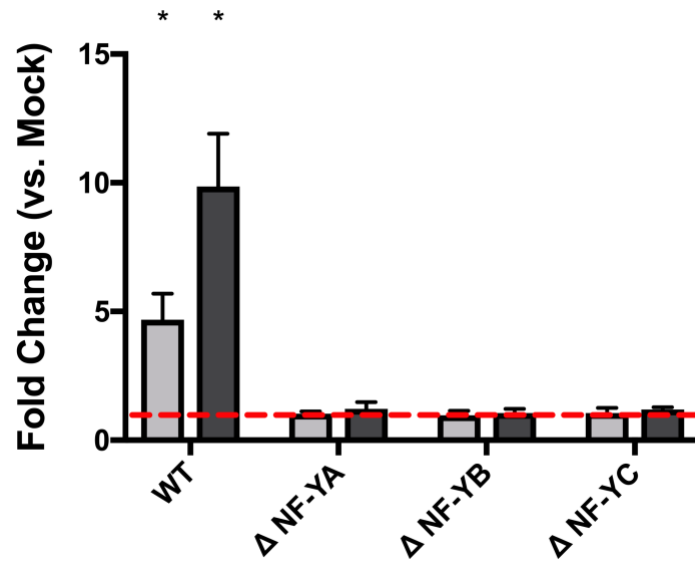


Figure S5. Induction time-course of NF-YA2, NF-YB2 and NF-YC3 effectors in yeast. Western blot analysis of **(A)** NF-YA2:HA, **(B)** NF-YB2:MYC, and **(C)** NF-YC3:FLAG accumulation in response to 10nM β -estradiol induction for 3, 6, and 9 hours. A single biological replicate was tested for protein accumulation using anti-HA, anti-Myc and anti-Flag antibodies. Ponceau S staining of the PVDF membrane prior to transfer was used to test loading control. The experiment was repeated twice with similar results.



808
809 **Figure S6. Activation of the DIMR system in effector cassettes with broken T2A**
810 **sites.** Point mutations were generated in the T2A sites between NF-YA / NF-YB, between
811 NF-YB / NF-YC, and in both T2A sites simultaneously. T2A sites were broken through a
812 proline to alanine mutation near the end of each T2A site, as previously described
813 (Beekwilder et al. 2014). Error bars represent 95% confidence intervals. Asterisks above
814 individual bars indicate statistical significance over matched mock-treated samples, as
815 determined through two-way ANOVA ($p < 0.01$). Brackets with asterisks indicate
816 significance between induced samples. ns, not significantly different.
817



818
819
820
821
822
823
824
825
826

Figure S7. Activation of the DIMR system in the absence of individual NF-Y effectors. NF-^{YA2/B2/C3} Effectors with empty components for NF-YA (Δ NF-YA), NF-YB (Δ NF-YB), or NF-YC (Δ NF-YC), were tested for ability to activate the 4x *FT* CCAAT box in the *ASN1*-based promoter. Error bars represent 95% confidence intervals. Asterisks above individual bars indicate statistical significance over matched mock-treated samples, as determined through two-way ANOVA ($p < 0.01$); all bars lacking asterisks were found to be nonsignificant compared to matched mock-treated samples.

- 827
828 Amoutzias GD, Robertson DL, Van de Peer Y, Oliver SG (2008) Choose your partners:
829 dimerization in eukaryotic transcription factors. *Trends in biochemical sciences* 33
830 (5):220-229
- 831 Anderson DW, McKeown AN, Thornton JW (2015) Intermolecular epistasis shaped the
832 function and evolution of an ancient transcription factor and its DNA binding sites.
833 *Elife* 4:e07864
- 834 Beekwilder J, van Rossum HM, Koopman F, Sonntag F, Buchhaupt M, Schrader J,
835 Hall RD, Bosch D, Pronk JT, van Maris AJ, Daran JM (2014) Polycistronic
836 expression of a beta-carotene biosynthetic pathway in *Saccharomyces cerevisiae*
837 coupled to beta-ionone production. *Journal of biotechnology* 192 Pt B:383-392.
838 doi:10.1016/j.jbiotec.2013.12.016
- 839 Blount BA, Weenink T, Ellis T (2012) Construction of synthetic regulatory networks in
840 yeast. *FEBS letters* 586 (15):2112-2121
- 841 Bourgarel D, Nguyen CC, Bolotin-Fukuhara M (1999) HAP4, the glucose-repressed
842 regulated subunit of the HAP transcriptional complex involved in the fermentation–
843 respiration shift, has a functional homologue in the respiratory yeast *Kluyveromyces*
844 *lactis*. *Molecular microbiology* 31 (4):1205-1215
- 845 Broach JR, Guarascio VR, Jayaram M (1982) Recombination within the yeast plasmid
846 2 μ circle is site-specific. *Cell* 29 (1):227-234
- 847 Calvenzani V, Testoni B, Gusmaroli G, Lorenzo M, Gnesutta N, Petroni K, Mantovani
848 R, Tonelli C (2012) Interactions and CCAAT-Binding of *Arabidopsis thaliana* NF-Y
849 Subunits. *PLOS ONE* 7 (8):e42902. doi:10.1371/journal.pone.0042902
- 850 Cao S, Kumimoto RW, Gnesutta N, Calogero AM, Mantovani R, Holt BF (2014) A distal
851 CCAAT/NUCLEAR FACTOR Y complex promotes chromatin looping at the
852 FLOWERING LOCUS T promoter and regulates the timing of flowering in
853 *Arabidopsis*. *Plant Cell* 26 (3):1009-1017. doi:10.1105/tpc.113.120352
- 854 Cao S, Kumimoto RW, Siriwardana CL, Risinger JR, Holt BF, III (2011) Identification
855 and Characterization of NF-Y Transcription Factor Families in the Monocot Model
856 Plant *Brachypodium distachyon*. *PLoS ONE* 6 (6):e21805
- 857 Crick F (1970) Central Dogma of Molecular Biology. *Nature* 227 (5258):561-563.
858 doi:10.1038/227561a0
- 859 Cunningham BC, Wells JA (1989) High-resolution epitope mapping of hGH-receptor
860 interactions by alanine-scanning mutagenesis. *Science* 244 (4908):1081-1085
- 861 Curran KA, Karim AS, Gupta A, Alper HS (2013) Use of expression-enhancing
862 terminators in *Saccharomyces cerevisiae* to increase mRNA half-life and improve
863 gene expression control for metabolic engineering applications. *Metabolic*
864 *engineering* 19:88-97. doi:10.1016/j.ymben.2013.07.001
- 865 Diamond MI, Miner JN, Yoshinaga SK, Yamamoto KR (1990) Transcription factor
866 interactions: selectors of positive or negative regulation from a single DNA element.
867 *Science* 249 (4974):1266-1272
- 868 Donati G, Gatta R, Dolfini D, Fossati A, Ceribelli M, Mantovani R (2008) An NF-Y-
869 dependent switch of positive and negative histone methyl marks on CCAAT
870 promoters. *PLoS ONE* 3 (4):e2066
- 871 Dorn A, Bollekens J, Staub A, Benoist C, Mathis D (1987) A multiplicity of CCAAT box-
872 binding proteins. *Cell* 50 (6):863-872

873 Edmondson DG, Smith MM, Roth SY (1996) Repression domain of the yeast global
874 repressor Tup1 interacts directly with histones H3 and H4. *Genes & development* 10
875 (10):1247-1259

876 Encode Project Consortium T, Birney E, Stamatoyannopoulos JA, Dutta A, Guigó R,
877 Gingeras TR, Margulies EH, Weng Z, Snyder M, Dermitzakis ET,
878 Stamatoyannopoulos JA, Thurman RE, Kuehn MS, Taylor CM, Neph S, Koch CM,
879 Asthana S, Malhotra A, Adzhubei I, Greenbaum JA, Andrews RM, Flicek P, Boyle
880 PJ, Cao H, Carter NP, Clelland GK, Davis S, Day N, Dhami P, Dillon SC, Dorschner
881 MO, Fiegler H, Giresi PG, Goldy J, Hawrylycz M, Haydock A, Humbert R, James
882 KD, Johnson BE, Johnson EM, Frum TT, Rosenzweig ER, Karnani N, Lee K,
883 Lefebvre GC, Navas PA, Neri F, Parker SCJ, Sabo PJ, Sandstrom R, Shafer A,
884 Vetriche D, Weaver M, Wilcox S, Yu M, Collins FS, Dekker J, Lieb JD, Tullius TD,
885 Crawford GE, Sunyaev S, Noble WS, Dunham I, Dutta A, Guigó R, Denoeud F,
886 Reymond A, Kapranov P, Rozowsky J, Zheng D, Castelo R, Frankish A, Harrow J,
887 Ghosh S, Sandelin A, Hofacker IL, Baertsch R, Keefe D, Flicek P, Dike S, Cheng J,
888 Hirsch HA, Sekinger EA, Lagarde J, Abril JF, Shahab A, Flamm C, Fried C,
889 Hackermüller J, Hertel J, Lindemeyer M, Missal K, Tanzer A, Washietl S, Korbel J,
890 Emanuelsson O, Pedersen JS, Holroyd N, Taylor R, Swarbreck D, Matthews N,
891 Dickson MC, Thomas DJ, Weirauch MT, Gilbert J, Drenkow J, Bell I, Zhao X,
892 Srinivasan KG, Sung W-K, Ooi HS, Chiu KP, Foissac S, Alioto T, Brent M, Pachter
893 L, Tress ML, Valencia A, Choo SW, Choo CY, Ucla C, Manzano C, Wyss C, Cheung
894 E, Clark TG, Brown JB, Ganesh M, Patel S, Tammana H, Chrast J, Henrichsen CN,
895 Kai C, Kawai J, Nagalakshmi U, Wu J, Lian Z, Lian J, Newburger P, Zhang X, Bickel
896 P, Mattick JS, Carninci P, Hayashizaki Y, Weissman S, Dermitzakis ET, Margulies
897 EH, Hubbard T, Myers RM, Rogers J, Stadler PF, Lowe TM, Wei C-L, Ruan Y,
898 Snyder M, Birney E, Struhl K, Gerstein M, Antonarakis SE, Gingeras TR, Brown JB,
899 Flicek P, Fu Y, Keefe D, Birney E, Denoeud F, Gerstein M, Green ED, Kapranov P,
900 Karaöz U, Myers RM, Noble WS, Reymond A, Rozowsky J, Struhl K, Siepel A,
901 Stamatoyannopoulos JA, Taylor CM, Taylor J, Thurman RE, Tullius TD, Washietl S,
902 Zheng D, Liefer LA, Wetterstrand KA, Good PJ, Feingold EA, Guyer MS, Collins FS,
903 Margulies EH, Cooper GM, Asimenos G, Thomas DJ, Dewey CN, Siepel A, Birney
904 E, Keefe D, Hou M, Taylor J, Nikolaev S, Montoya-Burgos JI, Löytynoja A, Whelan
905 S, Pardi F, Massingham T, Brown JB, Huang H, Zhang NR, Bickel P, Holmes I,
906 Mullikin JC, Ureta-Vidal A, Paten B, Seringhaus M, Church D, Rosenbloom K, Kent
907 WJ, Stone EA, Gerstein M, Antonarakis SE, Batzoglu S, Goldman N, Hardison RC,
908 Haussler D, Miller W, Pachter L, Green ED, Sidow A, Weng Z, Trinklein ND, Fu Y,
909 Zhang ZD, Karaöz U, Barrera L, Stuart R, Zheng D, Ghosh S, Flicek P, King DC,
910 Taylor J, Ameer A, Enroth S, Bieda MC, Koch CM, Hirsch HA, Wei C-L, Cheng J,
911 Kim J, Bhinge AA, Giresi PG, Jiang N, Liu J, Yao F, Sung W-K, Chiu KP, Vega VB,
912 Lee CWH, Ng P, Shahab A, Sekinger EA, Yang A, Moqtaderi Z, Zhu Z, Xu X,
913 Squazzo S, Oberley MJ, Inman D, Singer MA, Richmond TA, Munn KJ, Rada-
914 Iglesias A, Wallerman O, Komorowski J, Clelland GK, Wilcox S, Dillon SC, Andrews
915 RM, Fowler JC, Couttet P, James KD, Lefebvre GC, Bruce AW, Dovey OM, Ellis PD,
916 Dhami P, Langford CF, Carter NP, Vetriche D, Kapranov P, Nix DA, Bell I, Patel S,
917 Rozowsky J, Euskirchen G, Hartman S, Lian J, Wu J, Urban AE, Kraus P, Van
918 Calcar S, Heintzman N, Hoon Kim T, Wang K, Qu C, Hon G, Luna R, Glass CK,

- 919 Rosenfeld MG, Aldred SF, Cooper SJ, Halees A, Lin JM, Shulha HP, Zhang X, Xu
920 M, Haidar JNS, Yu Y, Birney* E, Weissman S, Ruan Y, Lieb JD, Iyer VR, Green RD,
921 Gingeras TR, Wadelius C, Dunham I, Struhl K, Hardison RC, Gerstein M, Farnham
922 PJ, Myers RM, Ren B, Snyder M, Thomas DJ, Rosenbloom K, Harte RA, Hinrichs
923 AS, Trumbower H, Clawson H, Hillman-Jackson J, Zweig AS, Smith K,
924 Thakkapallayil A, Barber G, Kuhn RM, Karolchik D, Haussler D, Kent WJ,
925 Dermitzakis ET, Armengol L, Bird CP, Clark TG, Cooper GM, de Bakker PIW, Kern
926 AD, Lopez-Bigas N, Martin JD, Stranger BE, Thomas DJ, Woodroffe A, Batzoglou S,
927 Davydov E, Dimas A, Eyras E, Hallgrímssdóttir IB, Hardison RC, Huppert J, Sidow A,
928 Taylor J, Trumbower H, Zody MC, Guigó R, Mullikin JC, Abecasis GR, Estivill X,
929 Birney E, Bouffard GG, Guan X, Hansen NF, Idol JR, Maduro VVB, Maskeri B,
930 McDowell JC, Park M, Thomas PJ, Young AC, Blakesley RW, Muzny DM,
931 Sodergren E, Wheeler DA, Worley KC, Jiang H, Weinstock GM, Gibbs RA, Graves
932 T, Fulton R, Mardis ER, Wilson RK, Clamp M, Cuff J, Gnerre S, Jaffe DB, Chang JL,
933 Lindblad-Toh K, Lander ES, Koriabine M, Nefedov M, Osoegawa K, Yoshinaga Y,
934 Zhu B, de Jong PJ (2007) Identification and analysis of functional elements in 1% of
935 the human genome by the ENCODE pilot project. *Nature* 447:799.
936 doi:10.1038/nature05874
937 <https://www.nature.com/articles/nature05874#supplementary-information>
938 Farré EM, Liu T (2013) The PRR family of transcriptional regulators reflects the
939 complexity and evolution of plant circadian clocks. *Current opinion in plant biology*
940 16 (5):621-629
941 Flagfeldt DB, Siewers V, Huang L, Nielsen J (2009) Characterization of chromosomal
942 integration sites for heterologous gene expression in *Saccharomyces cerevisiae*.
943 *Yeast* 26 (10):545-551. doi:10.1002/yea.1705
944 Gnesutta N, Kumimoto RW, Swain S, Chiara M, Siriwardana C, Horner DS, Holt BF,
945 Mantovani R (2017) CONSTANS Imparts DNA Sequence Specificity to the Histone
946 Fold NF-YB/NF-YC Dimer. *Plant Cell* 29 (6):1516-1532. doi:10.1105/tpc.16.00864
947 Griffiths S, Dunford RP, Coupland G, Laurie DA (2003) The evolution of CONSTANS-
948 like gene families in barley, rice, and Arabidopsis. *Plant physiology* 131 (4):1855-
949 1867
950 Gustafsson C, Govindarajan S, Minshull J (2004) Codon bias and heterologous protein
951 expression. *Trends in biotechnology* 22 (7):346-353.
952 doi:10.1016/j.tibtech.2004.04.006
953 Hwang Y-H, Kim S-K, Lee KC, Chung YS, Lee JH, Kim J-K (2016) Functional
954 conservation of rice OsNF-YB/YC and Arabidopsis AtNF-YB/YC proteins in the
955 regulation of flowering time. *Plant cell reports* 35 (4):857-865
956 Jayaram N, Usvyat D, Martin AC (2016) Evaluating tools for transcription factor binding
957 site prediction. *BMC bioinformatics*:1
958 John S, Sabo PJ, Thurman RE, Sung M-H, Biddie SC, Johnson TA, Hager GL,
959 Stamatoyannopoulos JA (2011) Chromatin accessibility pre-determines
960 glucocorticoid receptor binding patterns. *Nature genetics* 43 (3):264
961 Jolma A, Yin Y, Nitta KR, Dave K, Popov A, Taipale M, Enge M, Kivioja T, Morgunova
962 E, Taipale J (2015) DNA-dependent formation of transcription factor pairs alters their
963 binding specificity. *Nature* 527 (7578):384

- 964 Jones KA, Yamamoto KR, Tjian R (1985) Two distinct transcription factors bind to the
965 HSV thymidine kinase promoter in vitro. *Cell* 42 (2):559-572
- 966 Khalil AS, Collins JJ (2010) Synthetic biology: applications come of age. *Nature*
967 *Reviews Genetics* 11 (5):367
- 968 Khalil AS, Lu TK, Bashor CJ, Ramirez CL, Pyenson NC, Joung JK, Collins JJ (2012) A
969 synthetic biology framework for programming eukaryotic transcription functions. *Cell*
970 150 (3):647-658
- 971 Kim IS, Sinha S, de Crombrughe B, Maity SN (1996) Determination of functional
972 domains in the C subunit of the CCAAT- binding factor (CBF) necessary for
973 formation of a CBF-DNA complex: CBF- B interacts simultaneously with both the
974 CBF-A and CBF-C subunits to form a heterotrimeric CBF molecule. *Mol Cell Biol* 16
975 (8):4003-4013.
- 976 Kim JH, Lee S-R, Li L-H, Park H-J, Park J-H, Lee KY, Kim M-K, Shin BA, Choi S-Y
977 (2011) High cleavage efficiency of a 2A peptide derived from porcine teschovirus-1
978 in human cell lines, zebrafish and mice. *PloS one* 6 (4):e18556
- 979 Knop M, Siegers K, Pereira G, Zachariae W, Winsor B, Nasmyth K, Schiebel E (1999)
980 Epitope tagging of yeast genes using a PCR-based strategy: more tags and
981 improved practical routines. *Yeast* 15 (10B):963-972
- 982 Kotula L, Curtis PJ (1991) Evaluation of foreign gene codon optimization in yeast:
983 expression of a mouse IG kappa chain. *Bio/technology (Nature Publishing*
984 *Company)* 9 (12):1386-1389
- 985 Lickwar CR, Mueller F, Hanlon SE, McNally JG, Lieb JD (2012) Genome-wide protein–
986 DNA binding dynamics suggest a molecular clutch for transcription factor function.
987 *Nature* 484 (7393):251
- 988 Luke G, Escuin H, De Felipe P, Ryan M (2010) 2A to the fore - research, technology
989 and applications. *Biotechnology & genetic engineering reviews* 26:223-260
- 990 Luscombe NM, Laskowski RA, Thornton JM (2001) Amino acid-base interactions: a
991 three-dimensional analysis of protein-DNA interactions at an atomic level. *Nucleic*
992 *acids research* 29 (13):2860-2874
- 993 Mahony S, Pugh BF (2015) Protein–DNA binding in high-resolution. *Critical reviews in*
994 *biochemistry and molecular biology* 50 (4):269-283
- 995 Mclsaac RS, Oakes BL, Wang X, Dummit KA, Botstein D, Noyes MB (2013) Synthetic
996 gene expression perturbation systems with rapid, tunable, single-gene specificity in
997 yeast. *Nucleic acids research* 41 (4):e57. doi:10.1093/nar/gks1313
- 998 Mizuno T (2004) Plant response regulators implicated in signal transduction and
999 circadian rhythm. *Current opinion in plant biology* 7 (5):499-505
- 1000 Morgunova E, Taipale J (2017) Structural perspective of cooperative transcription
1001 factor binding. *Current Opinion in Structural Biology* 47:1-8
- 1002 Nardini M, Gnesutta N, Donati G, Gatta R, Forni C, Fossati A, Vornrhein C, Moras D,
1003 Romier C, Bolognesi M, Mantovani R (2013) Sequence-specific transcription factor
1004 NF-Y displays histone-like DNA binding and H2B-like ubiquitination. *Cell* 152 (1-
1005 2):132-143. doi:10.1016/j.cell.2012.11.047
- 1006 Nevoigt E, Kohnke J, Fischer CR, Alper H, Stahl U, Stephanopoulos G (2006)
1007 Engineering of promoter replacement cassettes for fine-tuning of gene expression in
1008 *Saccharomyces cerevisiae*. *Appl Environ Microbiol* 72 (8):5266-5273.
1009 doi:10.1128/aem.00530-06

- 1010 Oldfield AJ, Yang P, Conway AE, Cinghu S, Freudenberg JM, Yellaboina S, Jothi R
1011 (2014) Histone-fold domain protein NF-Y promotes chromatin accessibility for cell
1012 type-specific master transcription factors. *Mol Cell* 55 (5):708-722.
1013 doi:10.1016/j.molcel.2014.07.005
- 1014 Petroni K, Kumimoto RW, Gnesutta N, Calvenzani V, Fornari M, Tonelli C, Holt BF,
1015 3rd, Mantovani R (2012) The promiscuous life of plant NUCLEAR FACTOR Y
1016 transcription factors. *Plant Cell* 24 (12):4777-4792. doi:10.1105/tpc.112.105734
- 1017 Poelwijk FJ, Kiviet DJ, Weinreich DM, Tans SJ (2007) Empirical fitness landscapes
1018 reveal accessible evolutionary paths. *Nature* 445 (7126):383
- 1019 Reyes JC, Muro-Pastor MI, Florencio FJ (2004) The GATA family of transcription
1020 factors in Arabidopsis and rice. *Plant physiology* 134 (4):1718-1732
- 1021 Rodriguez-Martinez JA, Reinke AW, Bhimsaria D, Keating AE, Ansari AZ (2017)
1022 Combinatorial bZIP dimers display complex DNA-binding specificity landscapes.
1023 *Elife* 6:e19272
- 1024 Romier C, Cocchiarella F, Mantovani R, Moras D (2003) The NF-YB/NF-YC structure
1025 gives insight into DNA binding and transcription regulation by CCAAT factor NF-Y. *J*
1026 *Biol Chem* 278 (2):1336-1345
- 1027 Sabourin M, Tuzon CT, Fisher TS, Zakian VA (2007) A flexible protein linker improves
1028 the function of epitope-tagged proteins in *Saccharomyces cerevisiae*. *Yeast* 24
1029 (1):39-45. doi:10.1002/yea.1431
- 1030 Siefers N, Dang KK, Kumimoto RW, Bynum WE, Tayrose G, Holt BF (2009) Tissue-
1031 specific expression patterns of Arabidopsis NF-Y transcription factors suggest
1032 potential for extensive combinatorial complexity. *Plant Physiol* 149 (2):625-641.
1033 doi:10.1104/pp.108.130591
- 1034 Sinha S, Kim IS, Sohn KY, de Crombrughe B, Maity SN (1996) Three classes of
1035 mutations in the A subunit of the CCAAT-binding factor CBF delineate functional
1036 domains involved in the three-step assembly of the CBF-DNA complex. *Mol Cell Biol*
1037 16 (1):328-337
- 1038 Sinha S, Maity SN, Lu J, de Crombrughe B (1995) Recombinant rat CBF-C, the third
1039 subunit of CBF/NFY, allows formation of a protein-DNA complex with CBF-A and
1040 CBF-B and with yeast HAP2 and HAP3. *Proc Natl Acad Sci U S A* 92 (5):1624-1628
- 1041 Siriwardana CL, Gnesutta N, Kumimoto RW, Jones DS, Myers ZA, Mantovani R, Holt
1042 BF (2016) NUCLEAR FACTOR Y, Subunit A (NF-YA) Proteins Positively Regulate
1043 Flowering and Act Through FLOWERING LOCUS T. *PLoS Genet* 12 (12):e1006496.
1044 doi:10.1371/journal.pgen.1006496
- 1045 Sundseth R, MacDonald G, Ting J, King AC (1997) DNA elements recognizing NF-Y
1046 and Sp1 regulate the human multidrug-resistance gene promoter. *Mol Pharmacol* 51
1047 (6):963-971
- 1048 Tao Z, Shen L, Gu X, Wang Y, Yu H, He Y (2017) Embryonic epigenetic
1049 reprogramming by a pioneer transcription factor in plants. *Nature* 551:124.
1050 doi:10.1038/nature24300
- 1051 <https://www.nature.com/articles/nature24300#supplementary-information>
- 1052 Zambelli F, Pavesi G (2017) Genome wide features, distribution and correlations of
1053 NF-Y binding sites. *Biochimica et Biophysica Acta (BBA) - Gene Regulatory*
1054 *Mechanisms* 1860 (5):581-589. doi:<https://doi.org/10.1016/j.bbagr.2016.10.007>
- 1055